Prediction of Long-term Creep of Composites from Doubly-shifted Polymer Creep Data

EVER J. BARBERO*
Mechanical and Aerospace Engineering
West Virginia University, Morgantown, WV 26506-6106, USA

ABSTRACT: Environmental effects on the creep response of composites are of great interest because these materials are very sensitive to temperature and other environmental conditions. Short and long-term creep effects have been studied for composites under various environmental conditions, but most studies rely on experimental testing of particular laminates. Here, a novel micro-mechanical/laminate model is developed to predict the creep response of laminated polymer matrix composites from matrix creep data. Furthermore, a novel two-parameter superposition method is used to predict the long-term response of the polymer matrix as a function of two environmental parameters: moisture and temperature. The procedure used to compute the two shift factors is described. The resulting master curve can be used to predict the long-term properties of the matrix and for any temperature and humidity conditions. Once the matrix behavior is known, the micro-mechanical/laminate model allows for accurate prediction of long-term properties of arbitrary laminates for the same conditions.

KEY WORDS: PMC, creep, Analytical Modeling, Thermo Mechanical Testing, VARTM.

INTRODUCTION

POLYMER MATRIX COMPOSITES (PMC) display important viscoelastic behavior, which is sensitive to environmental effects (temperature, humidity [1], radiation [2], etc.). Short and long term creep effects have been studied experimentally, but very few models have been developed to predict long-term creep of laminated composite materials from short-term data. This study presents an approximate methodology to predict long-term creep of composite laminates from short-term constituent data. Two contributions are described. First, a doubly-shifted superposition method is developed to account for temperature and moisture conditions. Second, a combined micro-mechanics/laminate model allows us to predict laminate creep from constituent data. The predictions are validated with experimental data for relatively short times for which aging effects can

*E-mail: Ever.Barbero@mail.wvu.edu

0021-9983/09/19 2109–16 $10.00/0 DOI: 10.1177/0021998308098239

be neglected. Aging effects [3,4] and deviations from a thermorheologically complex material (TCM) behavior [5,6] are not considered in this study although they may effect the accuracy of the predictions for very long times. Because our intention is to develop a simple methodology that can be used for preliminary design, every effort was made to arrive at the simplest model. Experimental data is presented for neat resin (matrix) and laminated composites including continuous strand mat, unidirectional, and bidirectional stitched fabric layers. Neat resin samples were tested to obtain the matrix creep properties directly, without relying on back calculation using any micro-mechanics equations. Besides being economical, this method has the advantage that various matrices can be experimentally qualified for creep response under various environmental conditions (temperature, moisture, radiation) before fabricating any composite samples.

The correspondence principle [7] offers a powerful tool for modeling linearly viscoelastic materials; that is, when the viscoelastic behavior can be assumed to be independent of the stress level. Most structures are likely to operate in a known and relatively narrow range of stress values. The stress range is known because the sizing of members, and thus the level of stress is determined to satisfy requirements such as maximum deflections, fatigue limits, notched strength, and compression after impact, etc. Therefore, in preliminary design, it is convenient to use linear viscoelasticity at the known stress range rather than using complex nonlinear models [1,8–10]. Using the correspondence principle, most analytical tools developed for elastic materials can be used by taking a Laplace transform. This excludes iterative techniques (e.g., the self consistent method) and formulas containing empirical factors (e.g., Halpin–Tsai equations [11]) because the dependence of empirical factors as a function of time is unknown. In contrast, we use asymptotically exact micromechanics [12] without empirical correction factors, yielding analytical expressions, which facilitate the evaluation of the Laplace transform.

The creep behavior of any linearly viscoelastic material can be represented by empirical models such as the power law, Maxwell, Ideal solid, etc. [13,14]. These empirical models simply curve fit the experimental creep data. Once the creep behavior (shear, longitudinal, and transverse) of the composite is known from experiments [15], either at the layer or laminate level, several numerical methods exist to integrate the viscoelastic equations [16–20]. A problem encountered with these proposed models is that they rely on experimental data for a particular laminate. This means that an expensive experimental program needs to be completed before attempting the design of the structure. The experimental program is very expensive for composites because the need to consider various fibers and resin types, several values of fiber volume fraction, and a number of temperature and moisture conditions, etc. Furthermore, several types of tests are necessary to evaluate the creep behavior in shear as well as longitudinal and transverse directions [21]. The proposed procedure allows us to predict all the components of the creep compliance tensor from the elastic properties of the fibers and the matrix creep data only.

EXPERIMENTAL PROGRAM

Thirty-six different tests were performed, each with four replicates, for a total of 144 samples. In addition to neat resin samples, three laminates described in Tables 1 and 2 were tested. The four materials were tested in nine conditions, three temperatures (-12.2, 21.1, 65.6°C) and three relative humidity (0, 12, 80% RH). Temperature and moisture-concentration equilibrium were reached before testing on all samples. The laminates were

Table 1. Laminate constituents.

Laminate	Resin	Fiber	Fiber volume fraction	Nominal thickness (mm)
$[90/CSM)4]_S$	411–350	UM1810	68%	4.115
$[90/45/-45/CSM)3]_S$	411–350	TVM3408	44%	7.087
$[45/-45/CSM)2]_S$	411–350	CM5005	46%	6.058

Table 2. Fiber reinforcement architecture.

Fiber mat	90 (oz/yd^2)	45 (oz/yd^2)	−45 (oz/yd^2)	CSM (oz/ft^2)
UM1810	18			1.0
TVM3408	16	9	9	0.75
CM5005		25	25	0.50

fabricated using vacuum assisted resin transfer molding (VARTM), also known as SCRIMP. The matrix was Derakane 411-350 with cumene hydroperoxide (CHP) used as catalyst and cobalt naphthenate (CoNap) used as a promoter. The fabrics were supplied by Brunswick Technology Inc. The composites were fabricated by Hard Core DuPont using Derakane resin supplied by Dow Chemical.

The creep response at constant load is found by using a fixture that applies a dead load to a specimen placed inside a Cincinnati Sub Zero ZH-32 environmental chamber. The chamber has a temperature range of −40–190.6°C and a humidity range of 0–99% RH. The specimens are loaded through pins which allows for thermal expansion of the system and for the specimen to be aligned properly. The specimen is dog boned to ensure that the maximum creep region will be in the center of the specimen. The dimensions were selected to prevent creep or failure at the grip region for the neat matrix samples [22]. The composite specimens were fabricated with the same dimensions, which provided more than sufficient strength in the grip region.

A Micro Measurements CEA-13-250UN-120 strain gauge was mounted on the sample. Micro Measurements M-bond 200 adhesive was used to fasten the gauge to the specimens. An RTV coating (Dow Corning 3140 RTV) was applied over to protect the gauge from moisture. The system had a temperature range of −73.3 to 204.4°C up to 100% RH for continuous use in static measurements and has a strain limit of 5%. The strain gauge was wired for temperature and apparent thermal strain compensation [23]. Finally, the load was applied to the specimen by a crank mechanism, which allows for instantaneous loading.

The strength and elastic modulus were determined *a priori* by a quasi-static test in a universal testing system. During creep testing, the stress level was kept within the linearly elastic range of the stress–strain response. The tests were run until a well-defined secondary creep region developed. A time period of 4 h proved to be sufficient for all temperature and humidity conditions included in the experimental program.

The matrix was tested at a constant stress level approximately one quarter of the ultimate strength (11 MPa). Two sets of four specimens were tested at each environmental condition.

The creep response of the three laminates (Tables 1 and 2) experience less initial strain than the matrix, and the secondary creep rates of the laminates are lower in value compared to the matrix. The matrix was tested for 4 h and the laminates for 22 h at approximately one quarter of the ultimate strength of each laminate (9 and 29.6 MPa, respectively).

EMPIRICAL FIT OF CREEP DATA

The simplest method for representing creep compliance data is by using a power law, which for linear viscoelastic materials is:

$$J(t) - J_0 = J' t^n \tag{1}$$

where J_0 represents the initial compliance at $t = 0$, J' and n are fitted to the data by logarithmic linear regression. However, the most common representation used in engineering design is the Maxwell model, which has two parameters, the initial modified compliance $1/K$ and the creep rate $1/C$. The Maxwell model can be illustrated as a single series spring-dashpot system. The mathematical representation is given by:

$$J(t) = \frac{1}{K} + \frac{t}{C} \tag{2}$$

under constant applied stress σ_0. The Maxwell model does not fit well the primary creep region, but represents well the secondary creep region. Accurate modeling of the primary creep region is often not necessary in structural design because these effects occur over a short period of time compared to the service life of the structure. The parameter $1/C$ is the creep rate of the material and $1/K$ is the modified initial compliance. This model has been primarily used to describe metallic materials which display straight line secondary creep regions over very long periods of time. The use of this model to represent the response of polymer materials has been controversial, because a power law better represents the creep of polymers for relatively short times. For structural design, however, the main interest is on the response for long periods of time. Experimental data for both neat matrix and composites suggest that the Maxwell model provides a good representation for long times. Because of its simplicity compared to the power law, the Maxwell model is routinely used in design. The Maxwell–Voigt four-parameter model can be used if the primary creep region needs to be modeled accurately. For long values of time, the four-parameter model reduces to the two-parameter model. The ideal-solid model [14] can be used if long-term data is available to ascertain the asymptotic zero strain-rate at long times inherent to the model.

DOUBLY-SHIFTED SUPERPOSITION

The polymer is modeled as a thermorheologically complex material (TCM), with two time-dependent shift factors: horizontal and vertical (a_H and a_V). A modified power law is proposed to represent the viscoelastic response of polymer matrices at various temperature and humidity conditions:

$$J(t) - J_0(T, \phi) = J' \frac{1}{a_V} \left[\frac{t}{a_H} \right]^n \tag{3}$$

where $J_0(T, \phi)$ is the initial compliance as a function of temperature and relative humidity, J' and n are constants over the full range of temperature T and relative humidity ϕ.

The vertical and horizontal shift factors are assumed separable into temperature and humidity components as follows:

$$\begin{aligned} a_H &= a_T(T)a_\phi(\phi) \\ a_V &= b_T(T)b_\phi(\phi). \end{aligned} \tag{4}$$

Values for the temperature and humidity components of the shift factors were found for the nine environmental conditions tested, using two empirical models (Maxwell and Power Law), and four materials (neat resin and three laminates described in Tables 1 and 2).

All values of initial compliance $J_0(T, \phi)$ are known from the static tests at $t = 0$. The initial compliance J_0 was found from a static test at each temperature (reported in Figure 1) or as the ordinate at the origin ($1/K$ in Equation (2)) as a function of temperature and relative humidity, as reported in Figure 2.

To solve for the remaining variables, the first step is to choose a reference temperature and relative humidity (21.1°C and 12% in this article). At the reference state, all shift factors are equal to one. Then, the experimental data is fitted by Equation (3) with $a_T = a_\phi = b_T = b_\phi = 1$ to obtain the parameters J' and n. A linear regression is performed using on the log of Eqaution (1) to obtain the parameters J' and n for the matrix at the three environmental conditions. The quality of the approximation achieved with the Maxwell fit is illustrated in Figure 3.

In the second step the parameters J' and n are kept fixed while the experimental creep compliance data at various temperatures and reference relative humidity ϕ_{ref} is used to find

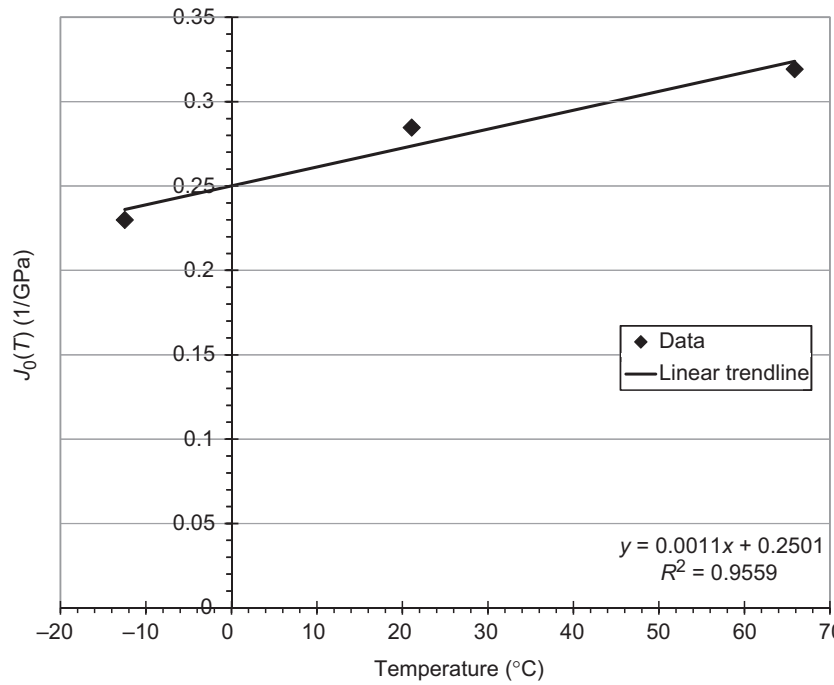

Figure 1. *Temperature dependency of the power-law initial compliance $J_0(T)$ of the matrix at 12% RH.*

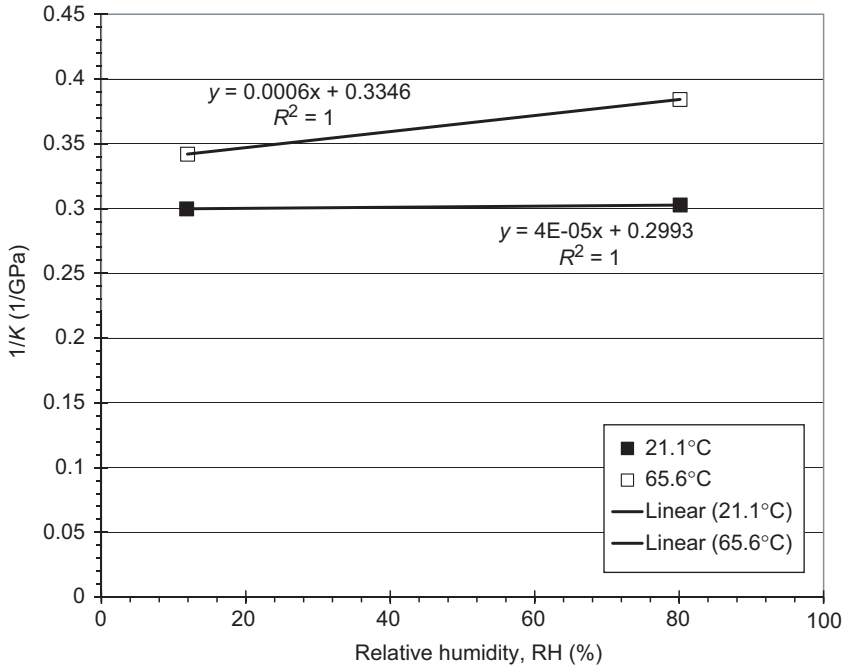

Figure 2. *Moisture and temperature dependency of the Maxwell initial compliance* $(K(T))^{-1}$.

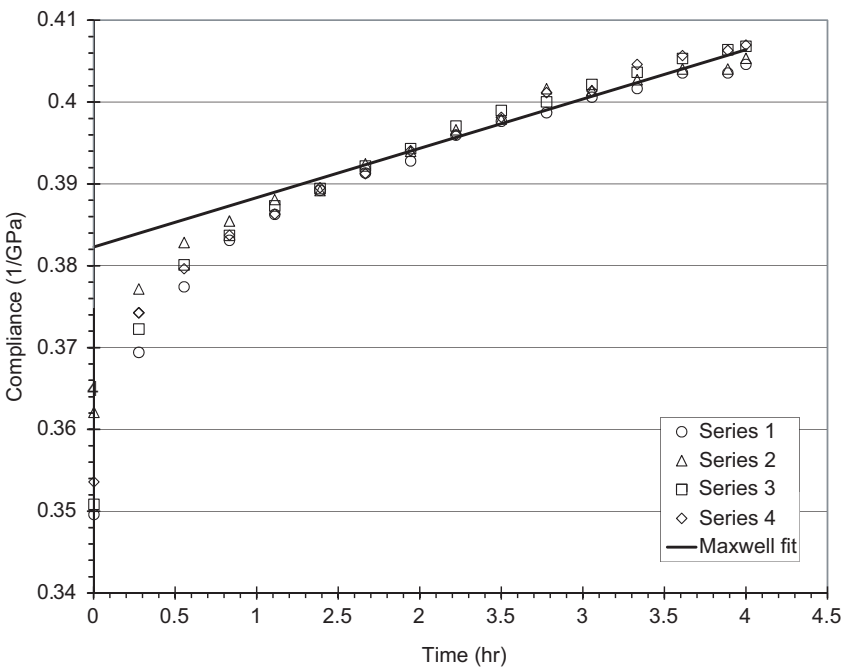

Figure 3. *Empirical fit of matrix creep data at 65.6°C, 80% RH.*

the temperature component of the horizontal and vertical shift factors a_T and b_T at each temperature for which data is available. Therefore, the values of $a_T(T)$ and $b_T(T)$ are found by minimizing the square of the error while $a_\phi = b_\phi = 1$; that is while the relative humidity is kept at its reference value. In this study, the temperature dependency was determined by using the data for various temperatures but at reference RH of 12% (Figures 4 and 5) and reported in Table 3.

Finally, the remaining data (for $\phi \neq \phi_{ref}$) is used to find the values of a_ϕ and b_ϕ by minimizing the error while keeping $a_T(T)$ and $b_T(T)$ unchanged. Then, the moisture dependency was found using the data at other values of RH. The combined shift factors are shown in Figures 6 and 7 and reported in Table 4.

The experimental data confirms that the matrix and composite shift factors are identical. Since the carbon fibers are elastic, they effect only the magnitude of the creep compliance, not the temperature and moisture dependency. That is, the combined horizontal and vertical shift factors a_H and a_V are equal for the matrix and for all the laminates analyzed (Tables 3 and 4). Furthermore, the experimental data confirms that the shift factors are independent of the empirical model used to fit the compliance data (Maxwell or Power Law). Therefore, if the master curve and the shift factor plot for the matrix is know, any laminate can be analyzed at any temperature and relative humidity condition. Still, the values of J_0, J', and n need to be predicted for the composite in terms of fiber and matrix properties, as explained in the next section.

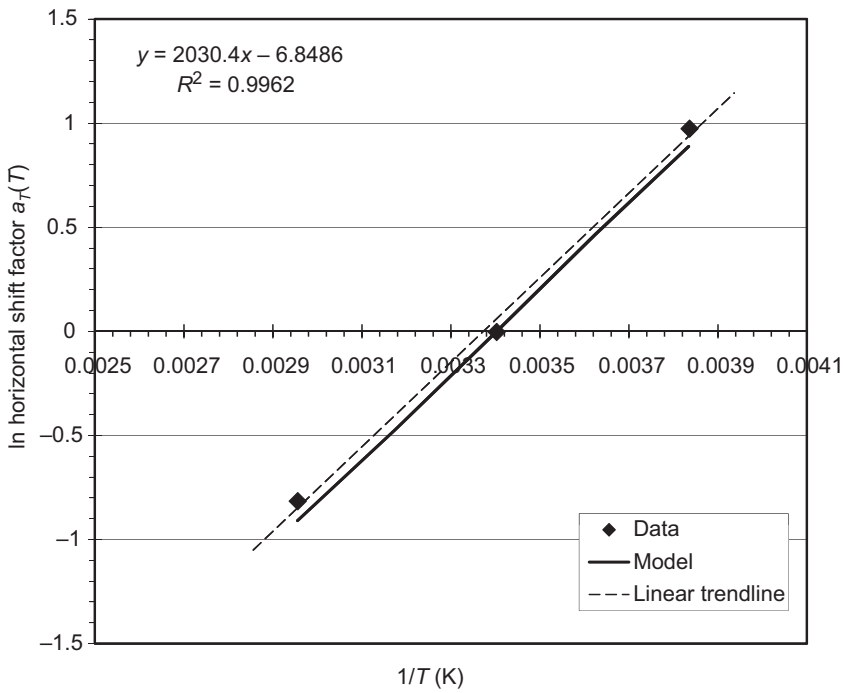

Figure 4. *Temperature dependency of the horizontal shift factor $a_T(T)$ at 12% RH.*

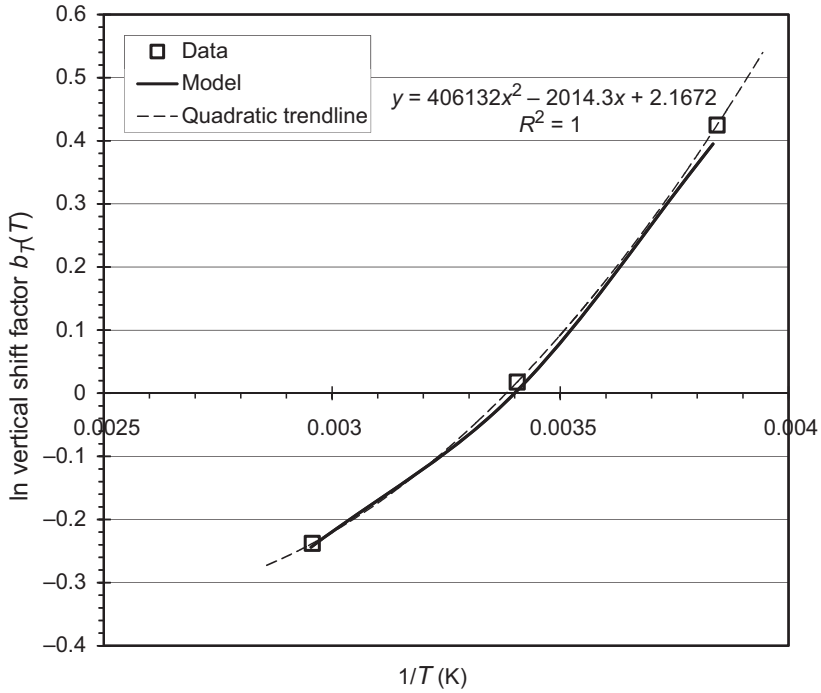

Figure 5. *Temperature dependency of the vertical shift factor $b_T(T)$ at 12% RH.*

Table 3. Temperature dependency of shift factors at each environmental condition.

Environment	a_T	b_T
12.2°C and 12% RH*	2.6835	1.4842
21.1°C and 12% RH	1	1
21.1°C and 80% RH	1	1
65.6°C and 12% RH	0.4415	0.7835
65.6°C and 80% RH	0.5462	0.4868

*At this temperature there is no practical distinction between 12% RH and 0% RH.

Laminate Model

Using the correspondence principle for linearly viscoelastic materials, the micromechanics formulas developed for elastic materials can be used directly in the Laplace domain, provided the formulas do not contain empirical parameters nor require iteration [24]. The equations are easier to manipulate using the Carson transform (indicated by $\widehat{L}$) instead, which is related to the Laplace transform (indicated by $\tilde{L}$) by:

$$\widehat{L}^*[f(t)] = s\,\tilde{L}^*[f(t)] \tag{5}$$

where $f(t)$ is any function of time.

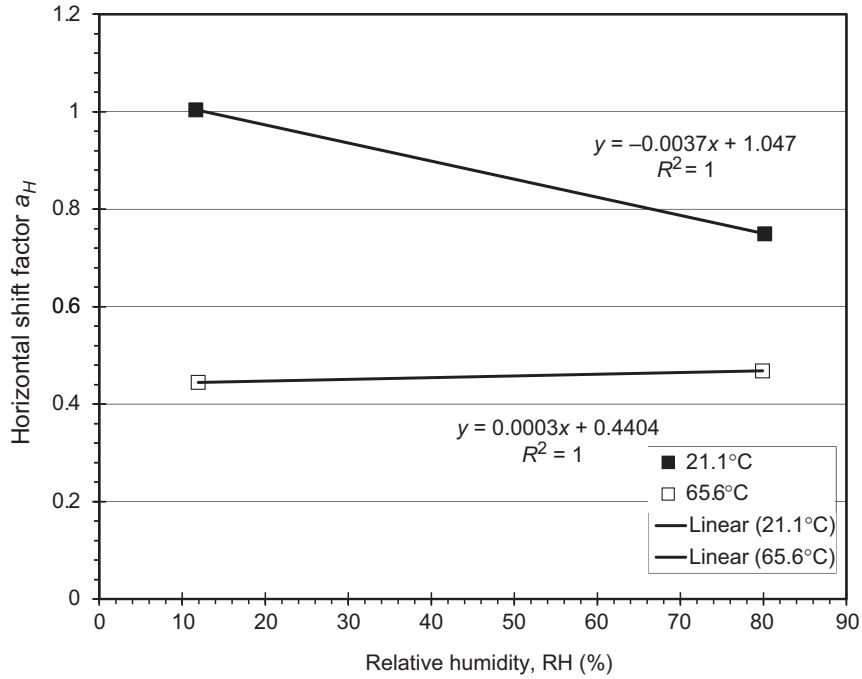

Figure 6. *Combined horizontal shift factor* $a_H = a_T a_\phi$.

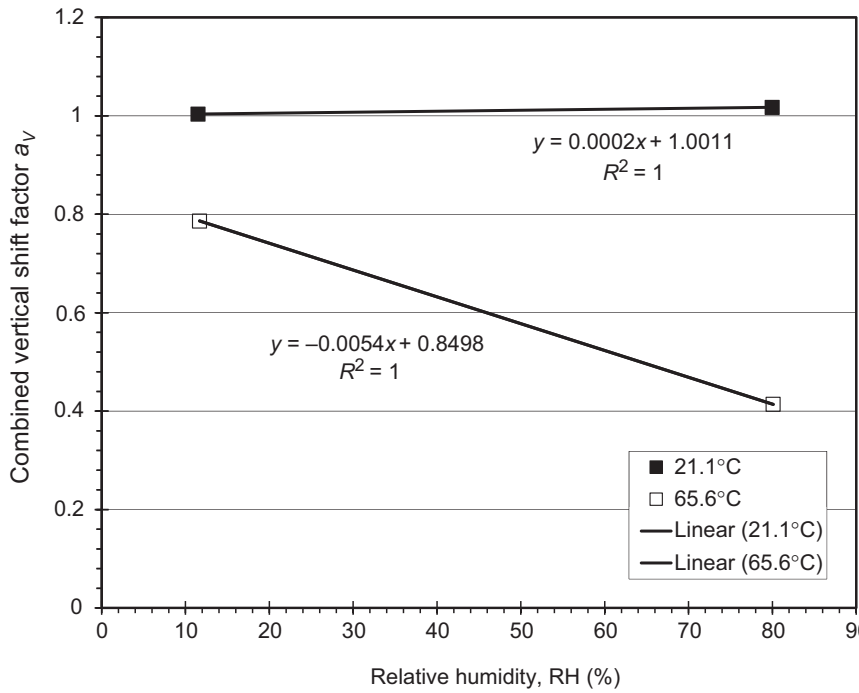

Figure 7. *Combined horizontal shift factor* $b_H = b_T b_\phi$.

Table 4. Combined shift factors at each environmental condition.

Environment	$a_T a_\phi$	$b_T b_\phi$
12.2°C and 12% RH*	2.6835	1.4842
21.1°C and 12% RH	1	1
21.1°C and 80% RH	0.7460	1.0108
65.6°C and 12% RH	0.4415	0.7835
65.6°C and 80% RH	0.4615	0.4112

*At this temperature there is no practical distinction between 12% RH and 0% RH.

The components of the relaxation tensor in the Carson domain for a unidirectional composite with periodically arranged fibers given in Ref. [12] as:

$$\begin{aligned}
\widehat{L}_{11}(s) &= \widehat{\lambda}_m + 2\widehat{\mu}_m - V_f \frac{\left[\begin{array}{c} S_3^2/\widehat{\mu}_m^2 - 2S_6S_3/\widehat{\mu}_m^2 g - aS_3/\widehat{\mu}_m\, c + \\ (S_6^2 - S_7^2)/\widehat{\mu}_m^2 g^2 + (aS_6 + bS_7)/\widehat{\mu}_m gc + (a^2 - b^2)/4c^2 \end{array}\right]}{D} \\
\widehat{L}_{12}(s) &= \widehat{\lambda}_m + V_f b \frac{\left[S_3/2c\,\widehat{\mu}_m - (S_6 - S_7)/2c\,\widehat{\mu}_m g - (a+b)/4c^2\right]}{D} \\
\widehat{L}_{23}(s) &= \widehat{\lambda}_m + V_f \frac{\left[aS_7/2\,\widehat{\mu}_m gc - (ba + b^2)/4c^2\right]}{D} \\
\widehat{L}_{22}(s) &= \widehat{\lambda}_m + 2\widehat{\mu}_m - V_f \frac{\left[-aS_3/2\,\widehat{\mu}_m c + aS_6/2\,\widehat{\mu}_m gc + (a^2 - b^2)/4c^2\right]}{D} \\
\widehat{L}_{44}(s) &= \widehat{\mu}_m - V_f \left[-\frac{2S_3}{\widehat{\mu}_m} + \left(\widehat{\mu}_m - \mu_f\right)^{-1} + \frac{4S_7}{\widehat{\mu}_m(2 - 2\nu_m)} \right]^{-1} \\
\widehat{L}_{66}(s) &= \widehat{\mu}_m - V_f \left[-\frac{S_3}{\widehat{\mu}_m} + \left(\widehat{\mu}_m - \mu_f\right)^{-1} \right]^{-1}
\end{aligned} \tag{6}$$

where:

$$\begin{aligned}
D = {} & \frac{aS_3^2}{2\,\widehat{\mu}_m^2 c} - \frac{aS_6S_3}{\widehat{\mu}_m^2 gc} + \frac{a(S_6^2 - S_7^2)}{2\,\widehat{\mu}_m^2 g^2 c} + \frac{S_3(b^2 - a^2)}{2\,\widehat{\mu}_m\, c^2} \\
& + \frac{S_6(a^2 - b^2) + S_7(ab + b^2)}{2\,\widehat{\mu}_m\, gc^2} + \frac{(a^3 - 2b^3 - 3ab^2)}{8c^3}
\end{aligned} \tag{7}$$

and

$$\begin{aligned}
a &= \mu_f - \widehat{\mu}_m - 2\mu_f\nu_m + 2\,\widehat{\mu}_m\,\nu_f \\
b &= -\hat{\mu}_m\nu_m + \mu_f\nu_f + 2\hat{\mu}_m\nu_m\nu_f - 2\mu_f\nu_m\nu_f \\
c &= (\hat{\mu}_m - \mu_f)(-\hat{\mu}_m + \mu_f - \hat{\mu}_m\nu_m - 2\mu_f\nu_m + 2\hat{\mu}_m\nu_f + \mu_f\nu_f + 2\hat{\mu}_m\nu_m\nu_f - 2\mu_f\nu_m\nu_f) \\
g &= (2 - 2\nu_m).
\end{aligned} \tag{8}$$

The series S_3, S_6, S_7 represent the geometry and spatial distribution of the inclusions. For circular cylindrical fibers, they are given in Ref. [12], as follows:

$$\begin{aligned} S_3 &= 0.49247 - 0.47603 V_f - 0.02748 V_f^2 \\ S_6 &= 0.36844 - 0.14944 V_f - 0.27152 V_f^2 \\ S_7 &= 0.12346 - 0.32035 V_f + 0.23517 V_f^2 \end{aligned} \tag{9}$$

were V_f is the fiber volume fraction and the Lamé constants are given by:

$$\begin{aligned} \widehat{\lambda}_m &= \frac{\widehat{E}_m \nu_m}{(1+\nu_m)(1-2\nu_m)} \\ \widehat{\mu}_m &= \frac{\widehat{E}_m}{2(1+\nu_m)}. \end{aligned} \tag{10}$$

where $\widehat{E}_m$, ν_m, and μ_m are the relaxation modulus, Poisson's ratio, and shear modulus of the matrix, E_f, ν_f, and μ_f are the elastic modulus, Poisson's ratio, and shear modulus of the fiber.

The Poisson's ratio of the matrix is constant over time, as confirmed experimentally for a broad frequency or temperature range except near the α and β polymer transitions [25]. The matrix data can be represented by any empirical model. To model a material with transverse isotropy, the following averaging procedure is used:

$$\widehat{C} = \frac{1}{\pi} \int_m^{\pi} [\overline{\Theta}^{(4)}][\widehat{L}][\overline{\Theta}^{(4)}]^T \mathrm{d}\theta \tag{11}$$

where $[\overline{\Theta}^{(4)}]$ is the fourth-order orthogonal rotational tensor (see Ref. [24,(1.40)]) representing a rotation θ about the x_1 axis (fiber direction). After completing the integration, the tensor $\widehat{C}$ is given by:

$$\begin{aligned} \widehat{C}_{11} &= \widehat{L}_{11} \\ \widehat{C}_{12} &= \widehat{L}_{12} \\ \widehat{C}_{22} &= \frac{3}{4}\widehat{L}_{22} + \frac{1}{4}\widehat{L}_{23} + \frac{1}{2}\widehat{L}_{44} \\ \widehat{C}_{23} &= \frac{1}{4}\widehat{L}_{22} + \frac{3}{4}\widehat{L}_{23} - \frac{1}{2}\widehat{L}_{44} \\ \widehat{C}_{66}(t) &= \widehat{L}_{66} \\ \widehat{C}_{44} &= \frac{1}{4}(\widehat{L}_{22} - \widehat{L}_{23} + 2\widehat{L}_{44}) \end{aligned} \tag{12}$$

where the new tensor is the averaged relaxation tensor for a transversely isotropic material. The relation between the relaxation tensor $[\widehat{C}]$ and the reduced relaxation matrix $[\widehat{Q}]$ for a unidirectional layer can be found by applying plain stress conditions $\sigma_3 = \sigma_4 = \sigma_5 = 0$ to

the compliance version of the constitutive equation [26]. As in classical lamination theory (CLT, [26]), the reduced relaxation coefficients are given by:

$$\begin{aligned}
\widehat{Q}_{11} &= \widehat{C}_{11} - \frac{\widehat{C}_{12}^2}{\widehat{C}_{22}} \\
\widehat{Q}_{12} &= \widehat{C}_{12}\left(1 - \frac{\widehat{C}_{23}}{\widehat{C}_{22}}\right) \\
\widehat{Q}_{22} &= \widehat{C}_{22} - \frac{\widehat{C}_{23}^2}{\widehat{C}_{22}} \\
\widehat{Q}_{66} &= \widehat{C}_{66}
\end{aligned} \tag{13}$$

where the reduced relaxation matrix $[\widehat{Q}]$ is symmetric. The plane-stress constitutive relationship for a unidirectional layer [26, (5.35)] can be rotated from the material coordinate system (1,2,6) to any other coordinate orientation using the classical transformation equations of CLT [26]. For a layer reinforced with randomly oriented fibers (such as continuous strand mat, chopped strand mat, etc.), we propose the following reduced relaxation matrix

$$\widehat{Q}^{CSM} = \frac{1}{\pi}\int_m^{\pi} [\Theta][\widehat{Q}][\Theta]^T \mathrm{d}\theta \tag{14}$$

where the rotation matrix $[\Theta]$ is given in Ref. [26]. In Equation (10), the stiffness matrix of a unidirectional layer $\widehat{Q}$ is rotated to every angle between 0 and π, added, and then divided by the interval π. This is an averaging procedure that yields the stiffness matrix of a layer with randomly oriented fibers$\widehat{Q}^{CMS}$. After completing the integral, the coefficients of the matrix are given by:

$$\begin{aligned}
\widehat{Q}_{11}^{CSM} &= \widehat{Q}_{22}^{CSM} = \frac{3}{8}\widehat{Q}_{11} + \frac{1}{4}\widehat{Q}_{12} + \frac{3}{8}\widehat{Q}_{22} + \frac{1}{2}\widehat{Q}_{66} \\
\widehat{Q}_{12}^{CSM} &= \widehat{Q}_{21}^{CSM} = \frac{1}{8}\widehat{Q}_{11} + \frac{3}{4}\widehat{Q}_{12} + \frac{1}{8}\widehat{Q}_{22} - \frac{1}{2}\widehat{Q}_{66} \\
\widehat{Q}_{66}^{CSM} &= \frac{1}{8}\widehat{Q}_{11} - \frac{1}{4}\widehat{Q}_{12} + \frac{1}{8}\widehat{Q}_{22} + \frac{1}{2}\widehat{Q}_{66} \\
\widehat{Q}_{16}^{CSM} &= \widehat{Q}_{26}^{CSM} = 0.
\end{aligned} \tag{15}$$

Next, a laminated composite material can be represented by applying classical lamination theory, but in the Carson domain. If the laminate is symmetric about the midplane surface, the relation between the stress resultants and strains is:

$$\begin{Bmatrix} \widehat{N}_x \\ \widehat{N}_y \\ \widehat{N}_{xy} \end{Bmatrix} = \begin{bmatrix} \widehat{A}_{11} & \widehat{A}_{12} & 0 \\ & \widehat{A}_{22} & 0 \\ \text{sym.} & & \widehat{A}_{66} \end{bmatrix} \begin{Bmatrix} \widehat{\varepsilon}_x \\ \widehat{\varepsilon}_y \\ \widehat{\gamma}_{xy} \end{Bmatrix} \tag{16}$$

with:

$$\widehat{A}_{ij} = \sum_{k=1}^{N_L} \widehat{Q}_{ij}^{(k)}\, t^{(k)} \tag{17}$$

where the superscript (k) indicates the layer number, $t^{(k)}$ is the layer thickness and N_L is the number of layers. Working in the Carson domain, the relaxation matrix $[\widehat{A}]$ is inverted analytically to obtain the creep compliance matrix:

$$[\widehat{\alpha}] = [\widehat{A}]^{-1}. \tag{18}$$

Both the relaxation and compliance matrices (Equation 17 and 18) are back-transformed to the time domain by a collocation method, which is explained in detail in Ref. [24, App. D]. The method provides N points for each coefficient of the creep compliance matrix $[\alpha(t)]$ ($N = 5$ was used in the examples). Two additional points can be obtained by using the limit value theorems [24, (7.44)]:

$$\begin{aligned} f(0) &= \lim_{s\to\infty}[sF(s)] \\ f(\infty) &= \lim_{s\to 0}[sF(s)]. \end{aligned} \tag{19}$$

Alternatively one might simply compute the elastic compliance of the laminate $[\alpha(t = 0)]$. The resulting $N + 2$ points can be fitted with the same empirical model used to fit the matrix creep data.

MODELING PREDICTIONS

With the combined shift factors given in Table 4 and the initial compliances given in Figures 1 and 2, it is possible to estimate the creep compliance of the matrix at any time, temperature, and RH using Equations (1) or (2). On the power law, $(J')^{-1} = 57.6\,\text{GPa}$ and $n = 0.2246$ for all conditions, while on the Maxwell model, $C = 854.4\,\text{GPa h}$.

The viscoelastic response of the composite was predicted following the procedure outlined earlier, in terms of the fiber elastic properties and the estimated matrix creep properties. The predicted composite compliance is compared in Figure 8 to actual composite experimental data, where it is noted that the model provides good predictive capability. Note that the comparison is good up to 22 h even though it is based on matrix data obtained over a 4 h period only. Furthermore, this model is unique in that it predicts all the components of the compliance and relaxation including shear and transverse properties.

CONCLUSIONS

A procedure to reduce experimental creep data using doubly-shifted superposition was presented. It is notable that identical shift-factors were found when the procedure was

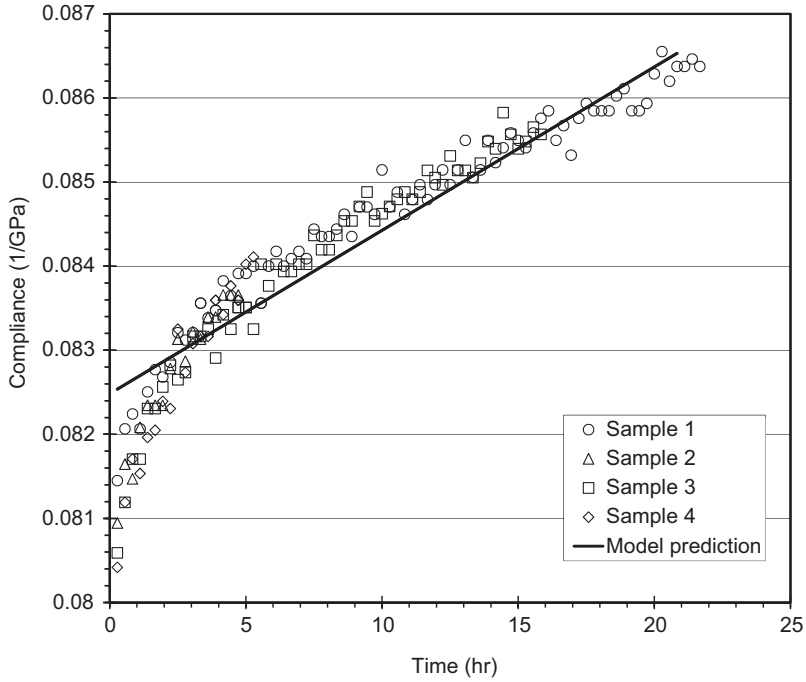

Figure 8. *Comparison at 21.1°C, 12% RH for* $[(90/45/-45/CSM)_3]_S$.

applied to creep data for matrix and three different laminates. Therefore, it is proven that only matrix data is required to model long-term compliance of arbitrary laminates. In this context, a novel micro-mechanical/laminate model was presented to predict compliance of arbitrarily laminated composites, which may include random and fabric reinforcement. Experimental matrix creep data is presented and used to predict laminate response. Then, laminate creep data is used to validate the prediction methodology, demonstrating a good predictive capability. Within the scope of this investigation, good agreement was achieved between the experimental data of three different laminates and the proposed model at short and long time response, even when the matrix creep behavior was experimentally characterized only for a short time.

NOMENCLATURE

$\widehat{\alpha}$ = in-plane compliance matrix
$\widehat{\varepsilon}$ = in-plane strain resultant array
λ_m, λ_f = Lame constant of the matrix and fiber, respectively
μ_m, μ_f = shear modulus of the matrix and fiber, respectively
ν_m, ν_f = Poisson's ratio of the matrix and fiber, respectively
ϕ, ϕ_0 = relative and reference relative humidity
Θ = 2D rotation tensor [26, (5.35)]
$\overline{\Theta}^{(4)}$ = 3D rotation tensor [24, (1.40)]
a_ϕ = humidity horizontal shift factor
a_H = horizontal shift factor

a_T = temperature horizontal shift factor
a_V = vertical shift factor
b_ϕ = humidity vertical shift factor
b_T = temperature vertical shift factor
k = layer number
t = time
$t(k)$ = layer thickness
$\widehat{A}$ = in-plane stiffness matrix
$\widehat{C}$ = transversely isotropic relaxation tensor in the Carson domain
E_m, E_f = relaxation modulus of the matrix and fiber, respectively
$J(t)$ = creep compliance
J_0 = initial creep compliance
J', n = parameters in the power law model
K, C = parameters in the Maxwell model
$\tilde{L}$ = relaxation tensor in the Laplace domain
$\widehat{L}$ = relaxation tensor in the Carson domain
$\widehat{N}$ = in-plane stress resultant array
N_L = number of layers in the laminate
$\widehat{Q}$ = 2D stiffness of a unidirectional layer
$\widehat{Q}^{CSM}$ = 2D stiffness of a continuous strand mat layer
T = temperature
V_f = fiber volume fraction

ACKNOWLEDGMENTS

The support provided by the West Virginia Department of Transportation Division of Highways under contract SPN T-699-PTP/BD-1 is acknowledged. The participation of M. Puckett from Dow Chemicals and K. Bernetich from HardCore DuPont is appreciated.

REFERENCES

1. Shen, C.H. and Springer, G.S. (1981). Effects of Moisture and Temperature on the Tensile Strength of Composite Materials, In: Springer, G.S. (ed.), *Environmental Effects on Composite Materials*, Vol. 1, pp. 79–93, Technomic Publishing Co. Inc., Westport, CT.
2. Yancey, R.N. and Pindera, M.J. (1990). Micromechanical Analysis of the Creep Response of Unidirectional Composites, *ASME Journal of Engineering Materials and Technology*, **112**: 157–163.
3. Struik, L.C.E. (1978). *Physical Aging in Amorphous Polymers and Other Materials*, Elsevier, Amsterdam.
4. Wang, J.Z., Parvatareddy, H., Chang, T., Iyengar, N., Dillard, D.A. and Reifsnider, K.L. (1995). Physical Aging Behavior of High Performance Composites, *Composites Science and Technology*, **54**: 405–415.
5. McCrum, N.G. (1992). The Interpretation of Physical Ageing in Creep and DMTA from Sequential Ageing Theory, *Plastics, Rubber and Composites Processing and Applications*, **18**: 181–191.
6. Guerdoux, L., Duckett, R.A. and Froelich, D. (1984). Physical Ageing of Polycarbonate and PMMA by Dynamic Mechanical Measurements, *Polymer Papers*, **25**: 1392–1396.
7. Aboudi, J. (1991). *Mechanics of Composite Materials*, Elsevier Science Publishers, Amsterdam, pp. 124–154.

8. Lou, Y.C. and Shapery, R.A. (1971). Viscoelastic Characterization of a Fiber Reinforced Plastic, *Journal of Composite Materials*, **5**(4): 208–234.
9. Schapery, R.A. (1967). Stress Analysis of Viscoelastic Composite Materials, *Journal of Composite Materials*, **1**: 228–267.
10. Schapery, R.A. (1974). Viscoelastic Behavior and Analysis of Composites Materials, In: Sendeckyj, G.P. (ed.), *Mechanics of Composite Materials*, Vol. 2, pp. 86–168, Academic Press, New York.
11. Halpin, J.C. and Sims, D.F. (1974). Methods for Determining the Elastic and Viscoelastic Response of Composite Materials, *Composite Materials*: *Testing and Design* (*Third Conference*), pp. 46–66, Williamsburg, VA.
12. Barbero, E.J. and Luciano, R. (1995). Micromechanical Formulas for the Relaxation Tensors of Linear Viscoelastic Composites with Transversely Isotropic Fibers, *International Journal of Solids and Structures*, **32**(13): 1859-1872.
13. Flugge, W. (1967). *Viscoelasticity*, Blaisdell Publishing Company, Waltham, MA.
14. Bradley, S.W., Bradley, W.L. and Puckett, P.M. (1998). Symposium on Limitations of Tests Methods for Plastics, *ASTM STP 1369*, Norfolk, VA.
15. Tuttle, M.E. and Brinson, H.F. (1985). Prediction of the Long-term Creep Compliance of General Composite Laminates, *Experimental Mechanics*, **6**(1): 89–102.
16. Dillard, D.A., Morris, D.H. and Brinson, H.F. (1981). Creep and Creep–rupture of Laminated Graphite-epoxy Composites, VPI&SU Report VPI-E-81-3, Blacksburg, VA.
17. Zhang, S.Y. and Xiang, X.Y. (1992). Creep Characterization of a Fiber Reinforced Plastic Material, *Journal of Reinforced Plastics and Composites*, **2**: 1187–1194.
18. Singhal, S.N. and Chamis, C.C. (1992). Environmental Effects on Long Term Behavior of Composite Laminates, *24th International SAMPE Technical Conference*, October, Anaheim, CA.
19. Kennedy, T.C. and Wang, M. (1994). Three-dimensional, Nonlinear Viscoelastic Analysis of Laminated Composites, *Journal of Composite Materials*, **28**: 902–923.
20. Lin, K.Y. and Hwang, I.H. (1989). Thermo-viscoelastic Analysis of Composite Materials, *Journal of Composite Materials*, **23**: 554–569.
21. Walrath, D.E. (1991). Viscoelastic Response of a Unidirectional Composite Containing Two Viscoelastic Constituents, *Experimental Mechanics*, **31**(2): 111–117.
22. Harris, J. and Barbero, E.J. (1998). Prediction of Creep Properties of Laminated Composites from Matrix Creep Data, *Journal of Reinforced Plastics and Composites*, **17**(4): 361–379.
23. Murry, W.M. and Miller, W.R. (1992). *The Bonded Electrical Resistance Strain Gage*, Oxford University Press, New York.
24. Barbero, E.J. (2007). *Finite Element Analysis of Composite Materials*, CRC, Boca Raton, FL.
25. Lakes, R.S. (1998). *Viscoelastic Solids*, CRC, Boca Raton, FL.
26. Barbero, E.J. (1998). *Introduction to Composite Materials Design*, Taylor & Francis, Philadelphia, PA.